Journal of Building Engineering 19 (2018) 592–601

Contents lists available at ScienceDirect

Journal of Building Engineering

journal homepage: www.elsevier.com/locate/jobe

Condensation at the exterior surface of windows

Anssi Laukkarinen*, Paavo Kero, Juha Vinha

Laboratory of Civil Engineering. Tampere University of Technology, Tampere, Finland

ARTICLE INFO

Keywords:
Building physics
Condensation
Energy efficiency
Heat transfer
Moisture transfer
Windows

ABSTRACT

New energy efficient windows have a higher risk for outdoor air vapour condensing to their exterior surface, when compared to older windows with lower thermal resistance. This external condensation can reduce visibility through the window, decrease owner satisfaction and affect the behaviour of window buyers and sellers. The purpose of this study was to analyse the impact of window U-value and other factors on the occurrence of external condensation. A combined heat and moisture transfer model was created and used for the calculations. According to the results, the duration and amount of external condensation are projected to increase in the future due to lower window U-values and climate change. Exterior surface emissivity, external shadings and building location had a big impact on the amount of yearly condensation hours, while window orientation and solar absorption coefficient had a smaller impact. There was also an interesting power-law-type correlation between yearly condensation hours and the median effective thickness of the condensation layer. The results help window manufacturers and building designers make more accurate decisions in their future work.

1. Introduction

1.1. Background

The energy efficiency of buildings is an important topic in building design. Well designed and implemented building energy efficiency measures have the potential to decrease life-cycle costs, increase local energy security and lower the environmental impacts from a building. On the other hand, incomplete measures might only increase investment costs, increase risks for different kinds of faults and eventually hamper user satisfaction. This means that ideally the design choices used to improve building energy efficiency should achieve the energy performance targets, while avoiding the possible negative consequences.

One essential use of energy in buildings is for space heating, of which a part is lost through windows. To reduce these heat losses, more energy efficient windows with higher thermal resistance are being developed and taken into use. This change in the thermal resistance of the windows means that their inside surfaces become warmer and the outside surfaces becomes colder. While this change reduces the risk of indoor air moisture condensing to the inside surfaces, it increases the risk for outdoor air moisture condensing to the outside surfaces (a.k.a. external condensation).

El Diasty & Budaiwi [7] list several negative effects that external condensation can have in an air-conditioned buildings in hot and humid climates: i) Alteration or hampering of visibility through the window, ii) Reduction of daylighting intensity to indoors, iii) Easier accumulation of dust layer on the window surface, iv) Possibility of stains, discolouration and other damages due to rolling water drops and v) Changes to building cooling load due to latent heat transfer. The list is well applicable to the cold climatic conditions also, which is the focus area of this study.

A questionnaire was done in central Sweden among homeowners, who had received government subsidies related to promoting building energy-efficiency [24]. According to the program conditions, also window retrofitting was included in the program terms, as long as the window U-value was equal to or lower than 1.2 W/(m^{2}K). According to the results, 98% of the installed windows had U-values of 1.1–1.2 W/(m^{2}K). The expected life span and the energy label of the window were reported to be the two most important factors for choosing a specific type of window (92% of the respondents), while 53% of the respondents said that having no or little condensation at the window surface was important to them. Among those respondents who had reported of being aware of more energy efficient windows than the limit value for the subsidiary (28% of the total), unattractive investment costs (43%) and the possibility of external condensation (31%) were reported as the two main reasons for not choosing more energy-efficient windows. Although 31% and 4% of the respondents had reported minor or severe external condensation respectively, 98% of the all the respondents reported that they had been satisfied with their new windows. Even from those homeowners who had reported severe external condensation, 95% were satisfied with their windows.

* Corresponding author.
E-mail addresses: anssi.laukkarinen@tut.fi (A. Laukkarinen), paavo.kero@fcg.fi (P. Kero), juha.vinha@tut.fi (J. Vinha).

https://doi.org/10.1016/j.jobe.2018.06.014
Received 23 March 2018; Received in revised form 25 June 2018; Accepted 26 June 2018
Available online 28 June 2018
2352-7102/

In the same questionnaire [24], the estimated lack of cost benefits and the increased risk for external condensation were the two main reasons, for the window sellers/installers not to generally promote more energy-efficient windows. This was directly reflected in the decisions made by the building owners, because they reported that the recommendations from the window sellers/installers had an important impact on their choice of window.

1.2. Literature review

The main idea of external condensation is, that when the temperature of the external surface is lower than the dew point temperature of the surrounding outdoor air, the extra vapour in the air will start condensing to the cold surface. The condensation process can be also described through air vapour content, so that the condensation process starts, when the vapour content of the surrounding air is higher than the saturation vapour content of the window surface. Longwave radiation is the main heat transfer mechanism, which can cause the exterior window surface temperature to decrease below the dew point (or frost point) temperature, making it an important parameter for the analysis [34].

Jonsson [18] has reported results from field measurements and modelling of external condensation. Comparison of three different windows with glazing U-values of 0.92, 1.13 and 1.85 W/(m^{2}K) gave results, that there was practically no external condensation with the window with the highest U-value. Of the two other windows, the amount of condensation hours was higher at the lower parts of the window compared to the top part of the window. There was 24–67 h of condensation per year at the window with U-value 1.13 W/(m^{2}K) and 68–166 h with U-value 0.92 W/(m^{2}K). The results were from the period 15 March – 31 December 1994 in Borås, Sweden.

In a study by Heimonen [13], the calculated amount of condensation hours started to increase sharply, when the center-of-glass U-value was lower than 0.6–0.7 W/(m^{2}K). The calculations considered the climatic conditions of Helsinki and Jyväskylä in Finland at the year 1979. The amount of condensation hours was in the order of 20–130 h for U-values of 0.55–0.8 W/(m^{2}K). The study mentions the impact of external shadings, surface emissivity, variation between successive years and different locations as important factors related to external condensation.

Jonsson [17] calculated both the total and daytime number of condensation hours with different U-values, view factors and years for the climatic conditions of Stockholm, Sweden. The number of condensation hours varied greatly between successive years, and most of the condensation appeared during the early mornings hours in the autumn. For the case with U-value 1.0 W/(m^{2}K) and view factor to the sky F = 0.5, the amount of condensation during 1988–1992 was 242–450 h per year, and the amount of daytime (07:00–19:00) condensation hours was 10–22% of the total amount. Yearly condensation hours generally increased with lower window U-value, larger view factor to the sky and lower local wind speed.

Low-emissivity coatings have been found to be able to reduce the occurrence of condensation in controlled field conditions [36] and in simulations [12,35]. The current practical lower limit for the emissivity of different coatings are currently around 0.15–0.20, but a substantial reduction in condensation hours have been found already for surface emissivity of 0.5 [35]. However, these coatings can also reduce the amount of visible light that is transmitted through the window, which can make the interiors darker ([4], p. 3). The low-emissivity coatings can also hamper the penetration of radio signals through the windows, causing problems in cell phone reception [2].

In Germany, Gläser & Ulrich [12] analysed the impact of low-emissivity coatings on the occurrence of external condensation. Based on their calculations, the authors concluded that by using the common low-emissivity coatings available in the market at the time ($\varepsilon_0 \approx 0.2$), it was possible to prevent frost and to some degree also dew from forming to the outside surface of vertical windows (in cases with $U_g \geq 0.47$ W/(m^{2}K)).

The use of hydrophobic coatings might not be able to prevent external condensation in all situations, but they can change the type of condensation layer. The change from dropwise to film-wise condensation layer can help maintain better visibility during condensation period [21,36].

It would be possible to create a time-dependent simulation model that would include the impacts of condensation, but in the previously mentioned studies the assumption of steady-state or quasi-steady-state conditions have been used. The results from El Diasty and Budaiwi [7] included interior surface temperature of a single-pane glazing, when there was condensation at the exterior surface. In the analysed situations, new temperature conditions were reached in approximately 15 min after a step change in boundary conditions. Windows with multiple panes should have longer time constants due to the higher heat capacity, but the assumption of quasi-steady-state conditions have been used also in this study.

As a summary of the literature review, the main factors related to the occurrence and prevention of external condensation is quite uniformly presented in the existing literature. However, the total number publications related to the topic is quite small, which causes a lack of more specific information related to the impacts and prevention measures of external condensation. Typically, exterior condensation is not seen as a dangerous phenomenon, but one that can harm the visibility through the window, be aesthetically unpleasant and in some cases, raise concern and questions of the functionality of the window. The topic is of interest for example for window manufacturers and sellers, building owners and building designers.

1.3. Steps and goals of this study

To get more detailed information related to the occurrence and prevention of external condensation, a group of calculations were done. Because condensation and evaporation of water vapour also affect the temperature conditions of windows, a combined heat and moisture calculation model was developed to describe the situation. The results from the developed model was compared qualitatively to the results from a simulation program IDA-ICE 4.7. After the accuracy and the behaviour of the model were considered adequate, sensitivity studies were performed related to different parameters.

The more specific research questions were: 1) How does the risk for external condensation change, when the energy efficiency of the windows (U-value) improves, and 2) What are the most effective measures for preventing or reducing the occurrence of external condensation?

2. Materials and methods

2.1. Balance equations and definitions

The conservation of energy requires that the net heat flow to a control volume is accounted for in the amount of energy stored in the control volume, when there are no heat sinks or sources. For the purposes of the study, the heat balance of the exterior window pane was written as Eq. (1). Incoming heat flows were assumed to have a positive sign.

$$C\frac{dT_{se}}{dt} = q_{i,se} + q_{conv} + q_{sw} + q_{lw} + q_{\nu}, \quad (1)$$

where C [J/(m^{2}K))] is the heat capacity of the control volume T_{se} [K] is the temperature of the exterior window surface, t [s] is the time, $q_{i,se}$ [W/m^2] is the heat flow from the indoors to the exterior surface, q_{conv} [W/m^2] is the convective heat flow from outdoor air to the exterior window surface, q_{sw} [W/m^2] is the heat flow by short wave radiation, q_{lw} [W/m^2] is the heat flow by long-wave radiation and q_{ν} [W/m^2] is the heat flow by vapour flow.

When using Eq. (1), it is assumed that the temperature of the outmost pane is the same as the temperature of the exterior surface and that the temperature can be described with a single nodal point. The heat flow density from indoors to the exterior surface was calculated with the help of the glazing (center-of-glass) U-value and the temperature difference over the window (Eq. (2)).

$$q_{i,se} = \frac{T_i - T_{se}}{\frac{1}{U_g} - R_{se}}, \tag{2}$$

where T_i [K] is the indoor temperature, U_g [W/(m^{2}K)] is the U-value of the glazing at the center of the window, from indoor air to outdoor air, R_{se} [m^{2}K/W] is the exterior surface resistance.

The glazing U-value can be calculated as the sum of thermal resistances according to SFS-EN 673 [27]. The exterior surface resistance is the reciprocal of the sum of the convective and radiative surface heat transfer coefficients according to SFS-EN ISO 6946 [30]. The convective and radiative surface heat transfer were treated separately in Eq. (1), but the heat flow from indoors was calculated using a constant external surface resistance (R_{se} = 0.04 m^{2}K/W). The heat flow by convection between the window surface and outdoor air was calculated using Eqs. (3)–(5).

$$q_{conv} = h_{conv} \cdot (T_e - T_{se}) \tag{3}$$

$$h_{conv} = 4 + 4v_{w,local} \tag{4}$$

$$v_{w,local} = 0.61 \cdot v_{w,airfield}, \tag{5}$$

where h_{conv} [W/(m^{2}K)] is the convective heat transfer coefficient, T_e [K] is the outdoor air temperature, $v_{w,local}$ [m/s] is the wind speed close to the surface, 0.61 is the calculated value of the roughness factor [26] and $v_{w,airfield}$ [m/s] is the wind speed at the meteorological weather station.

The convective surface heat transfer coefficient depends on the air speed (wind speed) close to the surface, but typically only open-field wind speed values from meteorological weather stations are known. Because of this, an approximate method was used, which is based on the standard [30]. The local wind speed next to the surface in Eq. (4) was calculated according to [26]. By assuming a village/suburban environment and a maximum height of five meters from the ground surface, a scaling factor (i.e. the roughness factor in SFS-EN 1991–1-4 [26]) of 0.61 was eventually used in the calculations, see Eq. (5). This calculation method does not take into account the exact air flow patterns around buildings. The calculation of incoming shortwave (solar) is shown in Eq. (6).

$$A_w q_{sw} = \alpha_{sw,w} \cdot \left(A_{sky} F_{sky,w} I_{dif,hor} + A_w I_{dir,0} + A_{gr} F_{gr,w} \tau_{sw,gr} I_{glob,hor} \right), \tag{6}$$

where A_w [m^2] is the window area, q_{sw} [W/m^2] is the absorbed short wave radiation, $\alpha_{sw,w}$ [-] is the shortwave absorptivity of the window pane, A_{sky} [m^2] is the area of the sky, [-] is the view factor from the sky to the window, $I_{dif,hor}$ [W/m^2] is the diffuse solar radiation to a horizontal surface, $I_{dir,0}$ [W/m^2] is the incoming direct solar radiation normal to the window, A_{gr} [m^2] is the area of the ground and other solid surroundings, $F_{ground,w}$ [-] is the view factor from the surrounding ground to the window, $\tau_{sw,gr}$ [-] is the shortwave reflectivity of the ground (i.e. the albedo) and $I_{glob,hor}$ [W/m^2] is the global radiation to a horizontal surface (sum of direct and diffuse solar radiation).

According to Incropera and others (2007, p. 812): *"The view factor $F_{i,j}$ is defined as the fraction of the radiation leaving surface i that is intercepted by surface j"*. The view factors are determined by the geometry of the situation. By using the reciprocity rule ($A_i F_{i,j} = A_j F_{j,i}$, ([16], p. 813)) for the sky and ground components and by dividing with the window area, Eq. (6) can be written as Eq. (7).

$$q_{sw} = \alpha_{sw,w} \cdot \left(F_{w,sky} I_{dif,hor} + I_{dir,0} + F_{w,gr} \tau_{sw,gr} I_{glob,hor} \right), \tag{7}$$

where $F_{w,sky}$ [-] is the view factor from the window to the sky and $F_{w,gr}$ [-] is the view factor from the window to the ground and other solid surroundings.

The diffuse radiation was assumed isotropic, which meant for the calculations that the walls facing north and south received the same amount of diffuse radiation. The direct solar radiation to a surface was calculated according to Eq. (8).

$$I_{dir,0} = max\left(0, \frac{I_{dir,hor}}{\cos\chi_z} \cos\chi_i\right), \tag{8}$$

where $I_{dir,hor}$ [W/m^2] is the direct solar radiation to a horizontal surface (calculated as the difference between global and diffuse radiation), χ_z [°] is the angle between the normal direction of the horizontal surface and the sun (i.e. the zenith angle, complementary to sun elevation angle) and χ_i [°] is the angle between the surface normal and the sun (i.e. the incidence angle).

In related to Eq. (8), additional conditions were used, that there was direct radiation to a surface only when the sun was above the horizon (the zenith angle was between $0 \leq \chi_z \leq 90°$) and the incidence angle was between $-90° \leq \chi_i \leq 90°$. The angles in Eq. (8) were calculated from Eq. (9) ([15], p. 15).

$$\begin{aligned} \cos\chi \;=\; & \sin\delta \sin L \cos s - \sin\delta \cos L \sin s \cos a \\ & + \cos\delta \cos L \cos s \cos h + \cos\delta \sin L \sin s \cos a \cos h \\ & + \cos\delta \sin s \sin a \sin h, \end{aligned} \tag{9}$$

where δ [°] is the declination, -23.45…23.45° depending on the time of the year, L [°] is the latitude, north positive, s [°] is the slope of the surface, 0° for a horizontal surface, 90° for a vertical surface, a [°] is the surface azimuth (south 0°, east 90°, north 180°, west -90°) and h [°] is the hour angle.

The declination and hour angle were calculated according to the equations presented in [1]. The net heat flow by long wave radiation was calculated according to Eq. (10).

$$q_{lw} A_w = \alpha_{lw,w} \left(A_{sky} F_{sky,w} \varepsilon_{sky} \sigma T_{sky}^4 + A_{gr} F_{gr,w} \varepsilon_{gr} \sigma T_{gr}^4 \right) - A_w \varepsilon_w \sigma T_{se}^4, \tag{10}$$

where $\alpha_{lw,w}$ [-] is the longwave absorptivity of the glass, equal to the longwave emissivity according to the Kirchhoff's law, ε_{sky} [-] is the sky emissivity for long-wave radiation, σ [W/(m^{2}K)] is the Stefan-Boltzmann constant, 5.67E-8W/(m^{2}K), T_{sky} [K] is the effective sky temperature, ε_{gr} [-] is the ground emissivity for long wave radiation (assumed equal to unity), T_{gr} [K] is the effective ground surface temperature (assumed equal to outdoor air temperature) and ε_w [-] is the long wave radiation emissivity (called hemispherical or total emissivity) of the exterior surface of the window.

By using the reciprocity rule and by dividing with the window area, Eq. (10) can be written as Eq. (11).

$$q_{lw} = \alpha_{lw,w} (F_{w,sky} \varepsilon_{sky} \sigma T_{sky}^4 + F_{w,gr} \varepsilon_{gr} \sigma T_{gr}^4) - \varepsilon_w \sigma T_{se}^4 \tag{11}$$

In this study, the downward longwave radiation from the atmosphere was determined by using semi-empirical models, which are typically based on the Stefan-Boltzmann equation. The semi-empirical models can be divided into two main categories, in which 1) The sky emissivity is set to unity and an effective sky temperature is determined from other variables, or 2) The sky temperature is set equal to outdoor air temperature and an effective sky emissivity is determined. When the method of effective sky temperature is used, the temperature difference between the outdoor air and the effective sky temperature is defined by Eq. (12).

$$T_{sky} = T_e + \Delta T, \tag{12}$$

where ΔT [K] is the temperature difference between the ground-level air temperature and the effective sky temperature.

The simulation program IDA-ICE uses a constant temperature difference of ΔT = -5 °C as a default value ([3], p. 10), which was used also as one case in this study. The international standard [29] gives the default value ΔT = -11 °C for intermediate climatic zones. For an outdoor air temperature of 278.15 K, sky temperature difference of −11 °C would correspond to an effective sky emissivity of $\varepsilon_{sky} = (1 + \Delta T/T_e)^4 = (1 - 11/278.15)^4 = 0.85$.

Besides values of constant temperature difference, the literature contains also more advanced semi-empirical models, which use typically available meteorological weather station data to calculate the downward longwave radiation [22,33,9]. Because it was not clear, which of the models would best describe the Finnish climatic conditions, multiple models were selected based on the results of the previously mentioned literature sources. Eqs. (13)–(15) present a model that is available in the TRNSYS simulation software ([31], Ch. 4.10.11, [23]).

$$T_{sky} = T_e(\varepsilon_{sky,clear}+0.8(1-\varepsilon_{sky,clear})C_{cover})^{0.25} \tag{13}$$

$$\varepsilon_{sky,clear} = 0.711 + 0.56\left(\frac{\theta_{dp}}{100}\right)+0.73\left(\frac{\theta_{dp}}{100}\right)^2 +0.013\cos\left(2\pi\frac{t_{hour}}{24}\right) + \frac{1.2p_0\left(\exp\left(\frac{\rho_0 gh}{p_0}\right)-1\right)}{100^2} \tag{14}$$

$$C_{cover} = \left(1.4286\frac{I_{dif,hor}}{I_{glob,hor}}-0.3\right)^{0.5}, \tag{15}$$

where $\varepsilon_{sky,clear}$ [-] is the clear sky emissivity according to Martin & Berdahl [23], C_{cover} [-] is a correction factor for the sky cloudiness, θ_{dp} [°C] is the dew point temperature in the outdoor air at ground level, t_{hour} [-] is the hour of the day (0−23), p_0 [atm] is the atmospheric pressure at sea level (1 atm), ρ_0 [kg/m^3] is the air density at sea level (1.27 kg/m^3), g [m^2/s] is the gravitational acceleration (9.81 m/s^2) and h [m] is the elevation above sea level.

The dew point temperature was calculated according to equations in SFS-EN ISO 13788 [28], which can be inverted to calculate saturation vapour pressure (Eq. (16)). The partial vapour pressure was converted to vapour content values in the calculations, using the ideal gas law.

$$p_{sat} = 610.5exp\left(\frac{17.269\theta}{237.3+\theta}\right) for\ \ \theta \geq 0°C$$
$$p_{sat} = 610.5exp\left(\frac{21.875\theta}{265.5+\theta}\right) for\ \ \theta<0°C, \tag{16}$$

where p_{sat} [Pa] is the saturation vapour pressure and θ [°C] is the air temperature.

Wallentén [33] has presented the Eq. (17) to calculate the sky emissivity, in which the coefficients have been calibrated for the Swedish climatic data. Eq. (17) includes the clearness index, to take into account the impact of variations in the atmosphere. Eqs. (18)–(19) include the calculation of the clearness index, which depends on the quotient between the measured amount of global radiation and the amount of extra-terrestrial radiation to a horizontal surface.

$$\varepsilon_{sky} = 1.547 + 0.598\left(\frac{\theta_{dp}}{100}\right)-0.569\left(\frac{T_e}{273.15}\right)-0.280K_0 \tag{17}$$

$$K_0 = \frac{I_{glob,hor}}{H_{hor}} \tag{18}$$

$$H_{hor} = rI_{sc}\cos(\chi_z), \tag{19}$$

where K_0 [-] is the clearness index, H_{hor} [W/m^2] is the amount of extra-terrestrial solar radiation on a horizontal surface, r [-] is the eccentricity correction factor, taking into account the yearly variation in the Earth's path around the Sun (0.96…1.04) and I_{sc} [W/m^2] is the solar constant, 1367 W/m^2.

Calculation of the eccentricity factor was calculated according to [37]. The hourly values of extra-terrestrial solar radiation to a horizontal surface (Eq. (19)) can be interpreted as the situation when there is no atmosphere present. The night-time values of the clearness index (and all similar indices in this study) were calculated based on hourly interpolation of morning and evening values. These two values for each day were calculated based on the cumulative sums of global and extra-terrestrial radiation separately, starting from the sunrise ($\chi_z < 90°$) until 12:00 mid-day and from 13:00 until the sun down ($\chi_z > 90°$). The average value was set to be at the middle of the morning and evening periods respectively. If the sun didn't rise at all, the default value of 0.5 was used for the clearness index.

Based on Flerchinger et al. [9], the downward longwave radiation was calculated with the equations by Dilley and O'Brien [6] clear-sky algorithm (Eqs. (21)–(22)), combined with the correction by Crawford and Duchon [5] for the cloudiness (Eqs. (20), (23), (24)). The model in Eqs. (20)–(24) is referenced to as the DOCD longwave radiation model later on in the text.

$$\varepsilon_{sky} = (1-s) + s\varepsilon_{sky,clear} \tag{20}$$

$$\varepsilon_{sky,clear} = \frac{1}{\sigma T_e^4}\cdot\left(59.38 + 113.7\left(\frac{T_e}{273.16}\right)^6 +96.96\sqrt{w/2.5}\right) \tag{21}$$

$$w = \frac{465(p_v/1000)}{T_e} \tag{22}$$

$$s = \frac{I_{glob,hor}}{S_{clr}} \tag{23}$$

$$S_{clr} = I_{sc}\cos(\chi_z)\tau_R\tau_{pg}\tau_w\tau_a, \tag{24}$$

where s [-] is the solar index, w [cm] is the amount of precipitable water in the atmosphere and τ_x [-] are the transmissions coefficients, given in Flerchinger et al. [9, app. A]. The heat transfer by condensation and evaporation was calculated according to Eq. (25).

$$q_v = L_v g_v, \tag{25}$$

where L_v [J/kg] is the latent heat of evaporation (2,260,000 J/kg) and g_v [kg/(m^{2}s)] is the density of the vapour mass flow between the exterior surface and the outdoor air. The mass flow in Eq. (25) was solved from Eq. (26).

$$\frac{\partial m}{\partial t} = g_v = \beta_v(\nu_e - \nu_{se}), \tag{26}$$

where m [kg/m^2] is the amount of water on the window surface, β_v [m/s] is the surface transfer coefficient for water vapour, ν_e [kg/m^3] is the vapour content of the outdoor air and ν_{se} [kg/m^3] is the vapour content of air at the exterior surface of the window. The surface transfer coefficient for water vapour (diffusion) was calculated from the convective heat transfer coefficient with the help of the Lewis equation (Eq. (27)) [14].

$$\beta_v = h_{conv}\cdot\left(\frac{\delta_{v,a}}{\lambda_a}\right), \tag{27}$$

where $\delta_{v,a}$ [m^2/s] is the vapour permeability of air (26E-6 m^2/s), ([16], app. A.8) and λ_a [W/(mK)] is the thermal conductivity of air (0.023 W/(mK)), ([16], app. A.4).

The surface coefficient and the amount of condensed moisture were calculated with hourly time steps. The heat transfer caused by mass transfer was calculated according to the following rules:

(1) If there was no pre-existing condensation at the window surface and the outdoor air vapour content was lower than the saturation vapour content at the surface, then there was no vapour transfer and also no heat transfer.
(2) Otherwise there was either pre-existing condensation at the surface or the conditions were susceptible for condensation. In this situation the relative humidity at the surface was assumed to be 100% RH and the vapour transfer was calculated according to Eq. (26).

The amount of latent heat transfer was solved as a part of the iteration loop for the solution and the amount of condensed moisture was stored as an initial value for the next time step.

In the numerical calculations, the temperature conditions were assumed to change in a quasi-steady-state manner in each hourly time step, which meant that the left-hand-side of Eq. (1) was set to zero. The coupled heat and moisture system was solved iteratively for each hourly time step according to the following algorithm:

(1) Initialize values and calculate the input data for the time step
(2) Calculate the right-hand side of Eq. (1). Because this value is directly linked to the time derivative of the unknown surface temperature, new temperature was calculated as the sum of the temperature of the previous iteration, plus a constant portion of the $C\frac{dT}{dt}$ -term ($T_{se,new} = T_{se,old}+0.01 \cdot C\frac{dT}{dt}$ was used).
(3) Re-calculate all the terms depending on the unknown surface temperature and iterate until the left-hand side of Eq. (1) is below a desired threshold (0.01 was used).

The parameters related to the numerical solution were chosen by testing different values and selecting the ones that seemed to provide converged results without excessive computation time.

2.2. Input data

The input data used in the calculations was originally received from the Finnish Meteorological Institute (FMI) and is described in Table 1.

The building physical test years have been selected based on the work reported by Ruosteenoja et al. [25] and Vinha et al. [32] and are available from the internet via FMI [10]. The background for the building energy simulation test years has been explained by Kalamees et al. [20] and Jylhä et al. [19] and they are available from FMI [11].

The outdoor air temperature and relative humidity from two meters height, global and diffuse radiation from a horizontal level and wind speed were utilized from the data sets in the calculations. The indoor air temperature was kept constant throughout the year (21 °C).

2.3. Interpretation of the results

The calculations related to Eqs. (1)–(27) include a large number of simplifications and possible error sources, due to the chosen mathematical model, variation in the input data, accuracy of the numerical solution and extensiveness of the calculated cases. The main limitations and sources for errors were considered to be:

- No air flows through or within the window
- Impacts of rain are not included
- Condensation or dirt doesn't affect surface radiative properties or the convective heat transfer coefficient
- Indoor air temperature stays constant throughout the year
- Solar radiation does not affect the surface temperature of the ground
- Steady-state conditions are assumed for each time step
- The material parameters or the window U-value do not depend on temperature
- Only vertical windows are analysed
- The impacts of different condensation mechanisms or possible run-off are not considered
- The impacts of external condensation on the visibility through the window are assessed only indirectly by using the indicators listed at the end of this section.

On the other hand the current model includes the impacts of both heat and vapour transfer, it includes all the main heat transfer mechanisms besides rain and air flows, it is fully documented and it is relatively easy to follow. To test the behaviour of the model, the results were compared to results from building simulation software IDA-ICE, which is widely used in Finland and which has been validated against several tests [8]. The both 'simple window' and 'detailed window' models of version 4.8 were used in the comparison simulations. Because the mathematical descriptions of the three models are different from each other, the comparison was done on a qualitative level, instead of e.g. trying to calibrate the models to produce as similar results as possible. The comparisons were done on a reference case, which was a south-facing window with a U-value of 1.0 W/(m^{2}K), surface emissivity of 0.837 and the solar absorption coefficient of 0.15. Downward longwave radiation was calculated according to the DOCD longwave radiation model. The view factor to the sky was 0.5. The same values were used also in all other calculations, if not otherwise specified.

The differences between results from different models were first analysed by visually comparing the differences between exterior window surface temperature and outdoor air dew point temperature. Especially the focus was on checking if the occasions when the surface temperature was below the outdoor air dew point temperature with different methods correlated to each other well. Finally, the root mean square error (RMSE) between the results from the three models were calculated.

The result data included the hourly vales of surface temperature (°C/K) and the amount of condensation (kg/m^2). When combined with the climate data, the following indicators were calculated for the presentation of the results:

(1) The total number of hours per year, when there is condensation at the window surface
(2) The number of daytime condensation hours per year, when there is condensation at the window surface between 6:00 in the morning and 21:00 in the evening
(3) The median value for the thickness of the condensed moisture, calculated from those hours, when there is condensation (the hourly values kg/m^2 divided by 1000 kg/m^3 and presented in micrometres (um)).

Table 1
The meteorological data sets used in the calculations.

General description	Additional information; Coordinates in decimals: °N, °E, m
30 years of hourly data from the reference period 1980–2009 and its projections to future climatic conditions of 2030, 2050 and 2100 ("30 year data")	Arctic Research Center of Finnish Meteorological Institute ("Sodankylä"); 67.37, 26.63, 179 Jyväskylä airport ("Jyväskylä"); 62.40, 25.68, 138 Jokioinen observatory ("Jokioinen"); 60.81, 23.50, 104 Helsinki-Vantaa airport ("Vantaa"); 60.33, 24.96, 51
Building physical test years ("BPTRY")	The hourly data is from the past years 2004 from Jokioinen (Finland) and 2007 from Vantaa (Finland) and from the corresponding years in the predicted future climatic conditions of 2030, 2050 and 2100.
Building energy simulation test years ("TRY")	The hourly one-year data is from the current reference period 1980–2009 and from the predicted future climatic conditions of 2030, 2050 and 2100 (average years). The data is from the climate zones IV (most northern, Sodankylä), III (middle Finland, Jyväskylä) and I-II (southern, Vantaa).

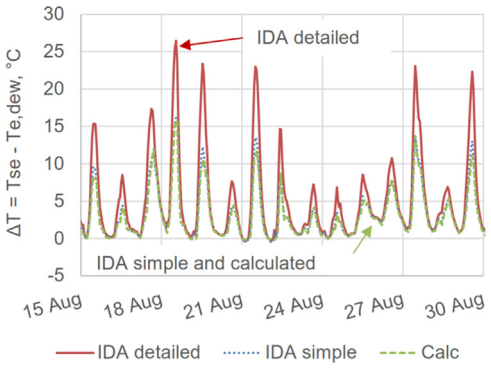

Fig. 1. Temperature difference between exterior surface temperature and outdoor air dew point temperature from the last two weeks of August from the test reference year Vantaa 2012. A typical example of the comparison results. The 'IDA detailed' and 'IDA simple' refer to the IDA-ICE simulation results, whereas 'calculated' refers to the equations presented in Section 2.1.

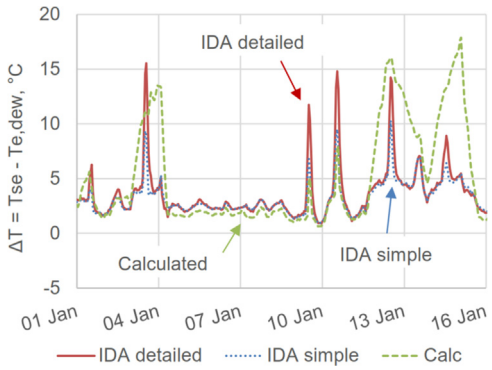

Fig. 2. Temperature difference between exterior surface temperature and the outdoor air dew point temperature from the first two weeks of the test reference year Vantaa 2012. The results contained a small number of events where the results deviated from the IDA-ICE results. The 'IDA detailed' and 'IDA simple' refer to the IDA-ICE simulation results, whereas 'Calculated' refers to the equations presented in Section 2.1.

3. Results and discussion

3.1. Comparisons to IDA-ICE results

Fig. 1 shows a typical example of the comparison results between different calculation methods.

The yearly average temperature difference between the exterior window surface and the outdoor air dew point was 6.3 °C for the IDA-ICE detailed window model, 4.7 °C for the IDA-ICE simple window model and 4.9 °C for the calculation method presented in chapter 2.1. The root mean square differences were 3.0 °C between the simple and detailed window models, 3.8 °C between chapter 2.1 and detailed window model and 2.0 °C between chapter 2.1 and simple window model. The differences between different models were biggest during the daytime and smaller during the night time. Also, it should be noted, that squaring the differences is especially affected by the peak values during the daytime, although the condensation hours occur during the night- and morning times. The temperature difference between the exterior surface temperature and the outdoor air dew-point temperature gave visually similar results, except that the daytime temperature peak of the exterior surface was clearly higher in the detailed IDA-ICE window model. The night-time temperature difference values were much closer to each other. At the beginning of the year, there were some bigger differences between the different calculation methods. Fig. 2 shows an example from January in test reference year Vantaa 2012.

The results were different from each other, which was also expected, because the mathematical models in each case were different from each other. The RMSE was quite big, but on the other hand there was no clear indication, which of the models would actually describe the physical phenomenon of external condensation in the most accurate way. On the positive side, the overall behaviour of the different models was similar to each other for the largest part of the year and the results were especially similar during the night time (highest probability for external condensation). The condensation risk hours occurred in similar times throughout the year, although the event duration between different models could typically vary 0–2 h per condensation event. In addition, the currently presented model allowed the inclusion of latent heat transfer and the track-keeping of the actual amount of condensed moisture. As a conclusion, the model presented in this paper was considered adequate for the current purposes and was used for further calculations.

3.2. Sensitivity studies

Fig. 3 shows the total amount of condensation hours for each year during 1980–2009 in Vantaa.

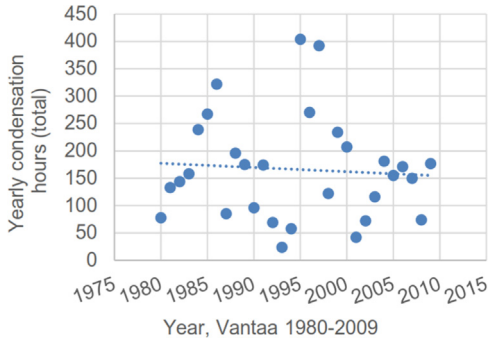

Fig. 3. Total amount of condensation hours in Vantaa during 1980–2009.

The total amount of condensation hours varied significantly between successive years in Vantaa 1980–2009 in Fig. 3 (between 24 and 404 h per year). The mean value was 166 h and standard deviation 94 h.

The difference between the north and south orientation was tested with the reference window in the current climate (Table 2).

The south oriented window experienced 11–64% more condensation hours than the north oriented window (Table 2). The main reason for this was, that as condensation typically occurs during the early morning hours of the summer and autumn months, the direct solar radiation hits the north-oriented window first when it rises above the horizon. The direct solar radiation warmed the north-oriented window during the critical hours and reduced the amount of condensation hours compared to south-oriented window.

Fig. 4 shows the impact of using different longwave radiation models. The values are 30-year average values.

Based on Fig. 4, using a constant temperature difference of −5 °C created the smallest amount of condensation hours, while using a constant temperature difference of −11 °C created the biggest. The three other tested models, which have their background in regression models of measured longwave radiation, created results that were relatively close to each other. Because the three more sophisticated models were fairly close to each other, the DOCD was selected for further calculations as it gave the biggest values of the three.

Fig. 5 shows the total average amount of condensation hours per year in different Finnish cities, as a function of the center-of-glass U-value.

According to Fig. 5, the total number of condensation hours per year increases as the center-of-glass U-value decreases. The amount of daytime condensation hours (6 − 21) was 24–43% of the total amount of condensation hours, the average being 32%. This means that although most of the condensation hours would occur during the night, there

Table 2
The difference in condensation hours between south and north orientation.

	Condensation hours (total)			Condensation hours (daytime)		
	South	North	Difference	South	North	Difference
Vantaa 1980–2009	166	147	13%	55	42	32%
Jokioinen 1980–2009	261	235	11%	91	74	23%
Jyväskylä 1980–2009	224	187	20%	69	49	42%
Sodankylä 1980–2009	47	33	43%	12	7	64%

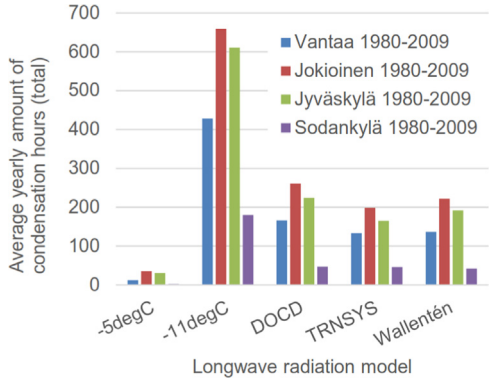

Fig. 4. The impact of using different models for downward longwave radiation.

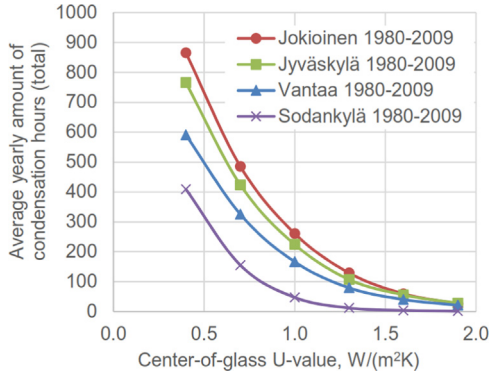

Fig. 5. The average yearly total amount of condensation hours per year in different Finnish locations, as a function of center-of-glass window U-value.

would be a non-negligible proportion of the condensation hours occurring during the time of the day, when people would be generally awake to see them. The results also show the importance of location on the occurrence of condensation: The average total condensation hours were smallest in the cold Northern Finland conditions, but maybe a little bit surprisingly the second lowest values were in climatic conditions of Helsinki-Vantaa airport, which is approximately 20 km north from the Gulf of Finland. The biggest amount of condensation hours occurred in the inland conditions of Jokioinen and Jyväskylä.

The amount of calculations could be reduced, if the 30-year data sets could be replaced with either the existing building physical or building energy simulation test years. Table 3 shows a comparison of total condensation hours between the different data sets for the reference case.

Based on Table 3, the building physical test year Jokioinen 2004 experienced a relatively large number of condensation hours, while the building physical test year Vantaa 2007 had a smaller-than-average amount of condensation hours. Because Jokioinen 2004 has been selected for structures that are mainly influenced by outdoor air relative humidity and the year Vantaa 2007 for structures that are mainly influenced by the driving rain, the results seem logical with regards to the building physical test years. However, the criticality of the building energy simulation test years varies from one climate zone to another, which makes the interpretation of the results more difficult. Based on the results in Table 3, the building physical test year Jokioinen 2004 could be used as a severe year also from the viewpoint of external condensation. However, because of the variation in the building energy simulation test years, the 30-year data sets were mainly used for throughout this study. Fig. 6 shows the impact of view factor from the window to the sky.

According to Fig. 6, the amount of condensation hours reduced practically to zero, if the view factor from the window to the sky was less than 0.2. A reduction in the view factor from 0.5 to 0.3 reduced the total condensation hours by roughly 90%. These values mean that eaves, trees, buildings and other external shadings can effectively reduce the amount of external condensation. The impact of exterior surface emissivity is shown in Fig. 7.

Based on Fig. 7, the occurrence of external condensation was almost completely removed, if the exterior surface emissivity was lower than 0.4. This is in line with the previous studies, which have concluded that it is not necessary to reach very low emissivity values (e.g. < 0.2) to prevent external condensation. Fig. 8 shows the impact of solar radiation absorption coefficient on the average total amount of condensation hours.

Based on the results in Fig. 8, the solar radiation absorption coefficient had some impact on the amount of condensation hours, but not as big as the window U-value, view factor to the sky or the exterior

Table 3
Comparison of energy simulation and building physical test years to 30-year reference period. n.a. = not available. Average total condensation hours per year in the reference case.

	ave	std	TRY	t = (TRY-ave)/std	BPTRY	t = (BPTRY-ave)/std
Vantaa 1980–2009	166	94	132	− 0.36	114	− 0.55
Jokioinen 1980–2009	261	144	132	− 0.89	402	0.98
Jyväskylä 1980–2009	224	128	239	0.12	n.a.	n.a.
Sodankylä 1980–2009	47	40	67	0.49	n.a.	n.a.

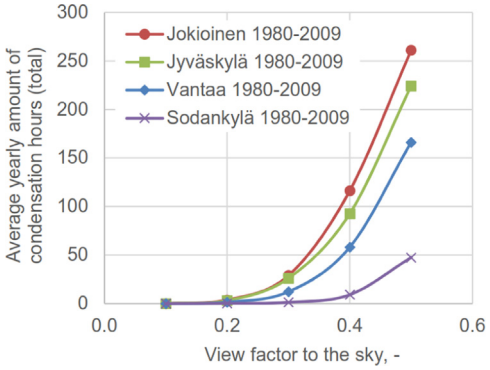

Fig. 6. The impact of view factor on the yearly average total amount of condensation hours.

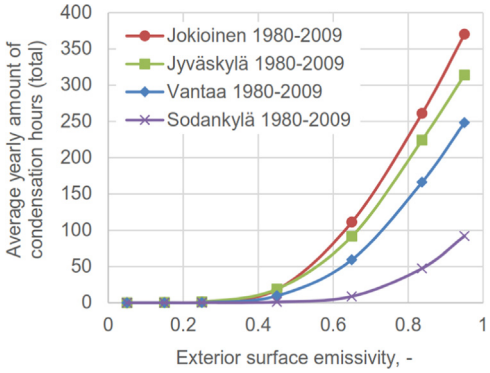

Fig. 7. The impact of exterior surface emissivity.

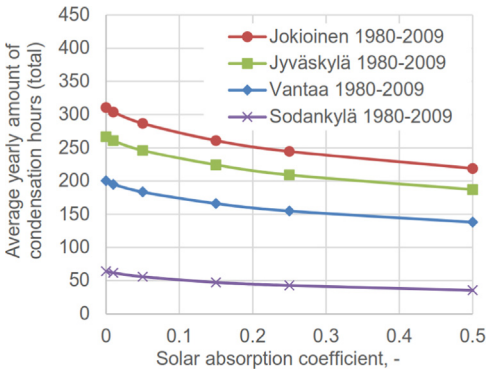

Fig. 8. The impact of solar absorption coefficient on the amount of condensation hours.

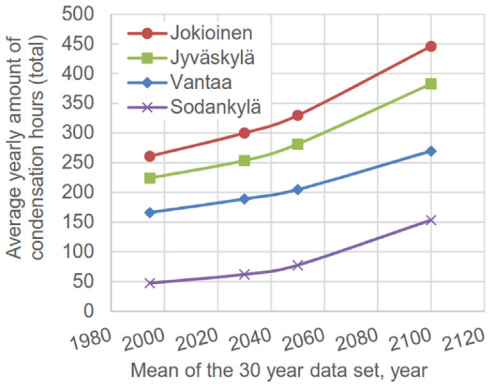

Fig. 9. The average total amount of condensation hours in the current and future climate.

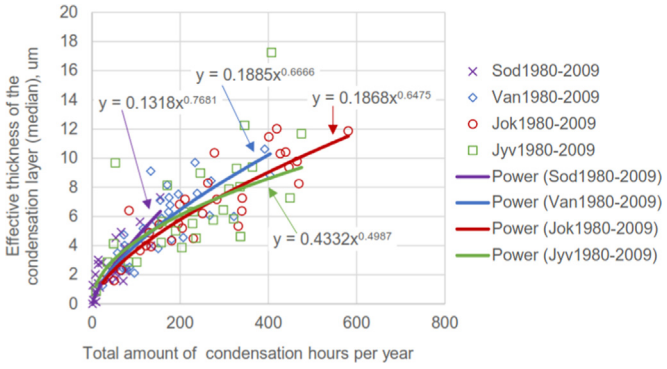

Fig. 10. The median thickness of the condensation layer in micrometres versus the total amount of yearly condensation hours. The thickness values are calculated from those hours, when there was condensation at the window surface.

surface emissivity. The impact was smallest in the northern part of Finland. Fig. 9 shows the impact of the predicted climate change on the average total amount of condensation hours.

In Fig. 9, the amount of condensation hours was higher in the future climatic conditions than in the current climate. The average total amount of condensation hours was 23–26% higher in the climatic conditions predicted for 2050, when compared to the current climatic conditions of southern and middle Finland. In northern Finland the increase was 64%, but this was also largely due to the much lower starting level. Fig. 10 shows the correlation between the median thickness of the condensation layer for hours with nonzero condensation thickness and the yearly total amount of condensation hours.

Based on Fig. 10, the median condensation layer thickness increased with increasing total amount of condensation hours per year. The behaviour was relatively similar regardless of the location. These results could also mean that there might have already been some amount of condensation hours in the existing windows, but the building users might have not noticed it due to the thin layer thickness. If the amount of condensation hours becomes bigger in the future, the condensation layer would be also more likely to become visible. If a model would be developed that would describe the impacts of effective condensation layer thickness to visibility, the correlations presented in Fig. 10 could be then used as a link between the architectural and structural design choices analysed in this article and the changes in visibility due to external condensation.

4. Conclusions

External condensation in windows means the process, where water vapour in the outdoor air condensates to the exterior window surface due to the low surface temperature. Based on the existing literature sources, one important consequence of this can be that the building owners might not want to invest for more energy-efficient windows because of the visual inconvenience or fear of mechanical degradation. In addition, building consultants might not want to promote these types of windows to avoid complaints from building owners. However, because an important part of space heating losses happens through windows, there is still a need to promote windows with lower U-values in the future.

To study the topic further, a single-point network model was created, which allowed the calculation of coupled heat and moisture conditions of the external surface in a quasi-steady-state manner. The results from the model were compared to the results from both simple and detailed window models in the IDA-ICE simulation software. The behaviour of the network model was considered adequate and so further parametric studies were conducted with it. The model was used to analyse the occurrence and influencing factors of moisture condensation at the exterior surface of vertical windows. The results behaved

consistently and were in line with the previous studies, which served also as an internal evaluation for the functioning of the calculation model. Although the current model included the coupled calculation of heat and moisture conditions on the window surface, there are still multiple simplifications that could be improved in future (see Section 2.3).

According to the results, both the improvements in the window U-value and the climate change increase the average yearly amount of condensation hours. Increased time duration was also linked to thicker effective condensation layer thickness, which means that without countering actions, in the future external condensation would be both more probable, and more visible.

External low-emissivity coatings had the capability to largely prevent external condensation. However, because some of the coatings can also prevent visible light entering room spaces and disturb cell phone signals, they can not be recommended without case-specific planning and implementation.

The use of shading towards the sky was an effective way reduce the yearly amount of condensation hours. Reaching a view factor of 0.2–0.3 from the window to the sky would clearly reduce the amount of condensation hours, compared to a non-shaded situation. Because external condensation happens largely during the early morning hours, shading solutions that allow the first available solar radiation to reach the window surface during the early morning hours would be preferable.

As a summary, the occurrence and visibility of external condensation on windows is predicted to increase in the future. This article has presented results that help window manufacturers and building designers to take the phenomenon into account when designing new window products and buildings. For the future research needs, it would be beneficial to define limit values or a classification system, that would connect the duration or the amount of external condensation to the actual visual disadvantages caused by it. Also in addition to simulations, laboratory and field tests should be used to evaluate the accuracy of the calculation results and to compare different window products in varying situations.

Acknowledgements

The earlier stages of the work were supported by the Finnish Funding Agency for Innovation (TEKES) under Grant number 2091/31/09; The Ministry of Environment under Grant number YM 45/612/2009; Confederation of Finnish Construction Industries RT; and three individual companies.

DisclosureDeclarations of interest

none.

References

[1] ASHRAE (2013), ASRAE Handbook. Fundamentals, SI Edition ed., ASHRAE, Atlanta, GA, USA.
[2] Asp, A., Baniya, A., Yunas, S.F., Niemelae, J. and Valkama, M. (2015), Applicability of Frequency Selective Surfaces to Enhance Mobile Network Coverage in Future Energy-Efficient Built Environments, Applicability of Frequency Selective Surfaces to Enhance Mobile Network Coverage in Future Energy-Efficient Built Environments, European Wireless 2015, pp. 1.
[3] A. Bring, P. Sahlin, M. Vuolle, Models for Building Indoor Climate and Energy Simulation, Kungl Tekniska Högskolan, Stockholm, Sweden, 1999.
[4] H. Bülow-Hübe, Energy Efficient Window Systems. Effects on Energy Use and Daylight in Buildings, Lund University, Lund Institute of Technology, Division of Energy and Building Design, P.O. Box 118, SE-221 00, Lund, Sweden, 2001.
[5] T.M. Crawford, C.E. Duchon, An improved parameterization for estimating effective atmospheric emissivity for use in calculating daytime downwelling longwave radiation, J. Appl. Meteorol. 38 (4) (1999) 474–480.
[6] A.C. Dilley, D.M. O'Brien, Estimating downward clear sky long-wave irradiance at the surface from screen temperature and precipitable water, Q. J. R. Meteorol. Soc. 124 (549) (1998) 1391–1401.
[7] R. El Diasty, I. Budaiwi, External condensation on windows, Construct. Build. Mater. 3 (3) (1989) 135–139 available at: ⟨http://www.sciencedirect.com/science/article/pii/0950061889900044 ⟩. (Accessed 11 November 2017)..
[8] EQUA, EQUA, IDA-ICE, validations & certifications, 2017. Available: ⟨https://www.equa.se/en/ida-ice/validation-certifications⟩ [2017, 28.11.].
[9] G.N. Flerchinger, W. Xaio, D. Marks, T.J. Sauer, Q. Yu, Comparison of algorithms for incoming atmospheric long-wave radiation, Water Resour. Res. 45 (2009) 13 (p. + 1 p. Erratum).
[10] FMI, The Finnish Building Physical Test Years , 2013. Available: ⟨http://ilmatieteenlaitos.fi/rakennusfysiikan-ilmastolliset-testivuodet⟩ [2017, 1 Dec].
[11] FMI, The Finnish Building Energy Simulation Test Years , 2011. Available: ⟨http://ilmatieteenlaitos.fi/rakennusten-energialaskennan-testivuosi⟩ [2017, 1 Dec].
[12] H.J. Gläser, S. Ulrich, Condensation on the outdoor surface of window glazing — Calculation methods, key parameters and prevention with low-emissivity coatings Thin Solid Films, Vol. 532, No. Supplement C, pp. 127–131. available at: ⟨http://www.sciencedirect.com/science/article/pii/S0040609013000369⟩. (Accessed 11 November 2017).
[13] I. Heimonen, Kondenssi ikkunoiden ulkopintaan [Condensation on the exterior surface of windows], 1997.
[14] H. Hens, Building Physics - Heat, Air and Moisture: Fundamentals and Engineering Methods with Examples and Exercises, 2nd ed., Wilhelm Ernst & Sohn Verlag fur Architektur und Technische, Berlin, GERMANY, 2012.
[15] Hens, H., Applied Building Physics. Boundary Conditions, Building Performance and Material Propertiestranslated by Anonymous Ernst & Sohn. A Wiley Company, Berlin, Germany, 2011.
[16] F.P. Incropera, D.P. DeWitt, T.L. Bergman, A.S. Lavine, Fundamentals of Heat and Mass Transfer, 6th ed, John Wiley & Sons, Hoboken, 2007.
[17] B. Jonsson, Calculating the occurrence of external condensation on high-performance windows, Borås, Sweden, 1999.
[18] B. Jonsson, Utvändig kondens på fönster. Mätningar i Borås 1994. SP Rapport 1995:01.
[19] K. Jylhä, J. Jokisalo, K. Ruosteenoja, K. Pilli-Sihvola, T. Kalamees, T. Seitola, H.M. Mäkelä, R. Hyvönen, M. Laapas, A. Drebs, Energy demand for the heating and cooling of residential houses in Finland in a changing climate, Energy Build. 99 (SupplementC) (2015) 104–116 available at: ⟨http://www.sciencedirect.com/science/article/pii/S0378778815002777 ⟩. (Accessed 1 December 2017).
[20] T. Kalamees, K. Jylhä, H. Tietäväinen, J. Jokisalo, S. Ilomets, R. Hyvönen, S. Saku, Development of weighting factors for climate variables for selecting the energy reference year according to the EN ISO 15927-4 standard, Energy and Buildings, Vol. 47, No. Supplement C, pp. 53–60. available at: ⟨http://www.sciencedirect.com/science/article/pii/S0378778811005779⟩. (Accessed 30 November 2017).
[21] A.J. Klemm, P. Klemm, K. Rozniakowski, G. Galbraith, Non-contact methods of measuring moisture concentration in external layers of building partitions. I—The influence of geometrical microstructure on the kinetics of moisture condensation on glass surfaces, Build. Environ. 37 (12) (2002) 1215–1220 available at: ⟨http://www.sciencedirect.com/science/article/pii/S0360132301001263 ⟩. (Accessed 15 June 2018)..
[22] M. Li, Y. Jiang, C.F.M. Coimbra, On the determination of atmospheric longwave irradiance under all-sky conditions, Sol. Energy 144 (2017) 40–48 available at: ⟨http://www.sciencedirect.com/science/article/pii/S0038092X17300154 ⟩. (Accessed 8 November 2017).
[23] M. Martin, P. Berdahl, Characteristics of infrared sky radiation in the United States, Sol. Energy 33 (3) (1984) 321–336.
[24] G. Nair, K. Mahapatra, L. Gustavsson, Implementation of energy-efficient windows in Swedish single-family houses, Applied Energy 89 (1) (2012) 321–336 available at: ⟨http://www.sciencedirect.com/science/article/pii/S0306261911004855 ⟩. (Accessed 11 November 2017)..
[25] K. Ruosteenoja, K. Jylhä, H. Mäkelä, R. Hyvönen, P. Pirinen, I. Lehtonen, Rakennusfysiikan testivuosien sääaineistot havaitussa ja arvioidussa ilmastossa: refi-b -hankkeen tuloksia, The Finnish Meteorologial Institute, Helsinki, Finland, 2013 (Data sets describing the current and future climatic conditions for building physical test years: Results from the REFI-B project).
[26] SFS-EN 1991-1-4, SFS-EN 1991-1-4:2011 + AC + A1 Eurocode 1: actions on structures. Part 1-4: general actions. Wind actions, The Finnish Standards Association SFS, Helsinki, Finland, 2011.
[27] SFS-EN 673, SFS-EN 673 Glass in building. Determination of thermal transmittance (U-value), Calculation method Finnish standards association SFS, Helsinki, Finland, 2011.
[28] SFS-EN ISO 13788, SFS-EN ISO 13788 Hygrothermal performance of building components and building elements. Internal surface temperature to avoid critical surface humidity and interstitial condensation. Calculation methods, The Finnish Standards Association SFS, Helsinki, Finland, 2013.
[29] SFS-EN ISO 52016-1, Energy performance of buildings. Energy needs for heating and cooling, internal temperatures and sensible and latent loads. Part 1: calculation procedurs (ISO 52016-1:2017), Finnish Standards Association SFS, Helsinki, Finland, 2017.
[30] SFS-EN ISO 6946, SFS-EN ISO 6946 Building components and building elements. Thermal resistance and thermal transmittance. Calculation methods, The Finnish Standards Association SFS, Helsinki, Finland, 2017.
[31] TRNSYS 17, TRNSYS 17: a Transient system simulation program. Volume 4: mathematical reference, Solar EnergyLaboratory, University of Wisconsin-Madison, 2009.
[32] J. Vinha, A. Laukkarinen, M. Mäkitalo, S. Nurmi, P. Huttunen, T. Pakkanen, P. Kero, E. Manelius, J. Lahdensivu, A. Köliö, K. Lähdesmäki, J. Piironen, V. Kuhno, M. Pirinen, A. Aaltonen, J. Suonketo, Ilmastonmuutoksen ja lämmöneristyksen lisäyksen vaikutukset vaipparakenteiden kosteusteknisessä toiminnassa ja rakennusten energiankulutuksessa [Effects of climate change and increasing of thermal insulation on moisture performance of envelope assemblies and energy consumption of buildings] Report nr. 159 Tampere University of Technology. Department of Civil Engineering. Report in Finnish, abstract in english.
[33] P. Wallentén, The Treatment of Long-Wave Radiation and Precipitation in Climate Files for Building Physics Simulations, The Treatment of Long-Wave Radiation and Precipitation in Climate Files for Building Physics Simulations, Thermal

Performance of the Exterior Envelopes of Whole Buildings XIII International Conference, Clearwater Beach, Florida, 2010.
[34] A. Werner, External Water Condensation and Angular Solar Absorptance: Theoretical Analysis and Practical Experience of Modern Windows, Uppsala University, 2007.
[35] A. Werner, A. Roos, Simulations of coatings to avoid external condensation on low U-value windows, Opt. Mater. 30 (6) (2008) 968–978.
[36] A. Werner, A. Roos, Condensation tests on glass samples for energy efficient windows, Sol. Energy Mater. Sol. Cells 91 (7) (2007) 609–615 available at: 〈http://www.sciencedirect.com/science/article/pii/S0927024806004570〉. (Accessed 11 November 2017).
[37] L.T. Wong, W.K. Chow, Solar radiation model, Appl. Energy 69 (3) (2001) 191–224 available at: 〈http://www.sciencedirect.com/science/article/pii/S0306261901000125〉. (Accessed 28 November 2017)..